



# Determining the Blind faults in Banesh Plain using Special Geoelectrical resistivity method

*Raheleh Farhang<sup>1</sup>, Abdolmajid Asadi<sup>2</sup>, Kouros Yazdjerdi<sup>3</sup>, Mohsen Pourkermani<sup>4</sup>*

*Received: 29 January 2022/ Revised: 01 March 2023/ Accepted: 12 April 2023/ Published: 01 June 2023*  
© Islamic Azad University (IAU) 2023

## Abstract

Knowledge of the blind faults location and revealing fault length in urban areas are so critical. Moreover, recognizing and direct study of faults location calls for selecting a proper approach to study the faults due to areas being covered with thick quaternary sediments and lack of faults outcrop in many areas. In doing so, one of the commonest methods is using geophysical methods. The study explored the blind faults of Banesh Plain in Fars, Iran using geoelectrical sampling with Schlumberger array and integrating it with field sampling and direct observations. Accordingly, 30 soundings and 10 profiles were developed in this regard and sections and pseudo-sections were analyzed. The results showed the existence of two fault zones along the northeast -southwest and northwest- southeast, and it seems that the conduction of groundwater in the mentioned area is under the influence of these two main zones.

**Keywords:** Banesh Beyza, Blind faults, Fars, Geoelectrical, Iran, Schlumberger array.

## Introduction

Given its special tectonic status with active basement faults, seismic margins, and the continuation of nontectonic movements, seismotectonics of the Zagros is among the areas with high seismic potential. Since there are widespread urban areas across this state and as most of the earthquakes are due to faults activity, the exact identification of the fault location, especially the blind ones, is so critical. Thus, the selection of identification methods leading to fast, reliable and low cost results is considered accordingly. Geophysical methods are of the

tools for identifying sub-surface structures. In fact, geophysical methods are a response to differences in the physical properties of rocks and the measurements to study the geology of the study area (Telford et al., 1988).

Since reach the lower parts is impossible due to sedimentary cover, indirect geophysical methods bring about the identification of the fractures and faults (Azadi et al., 2010). The ability of geophysical methods for deduction is of great importance, so that studies at a special distance without touching the ground can also lead to gathering information, which is a form of remote sensing science (Takahashi, 2014).

---

<sup>1</sup> Department of Geology, Fars Science and Research branch, Islamic Azad University, Fars, Iran & Department of Geology, Shiraz Branch, Islamic Azad University, Shiraz, Iran.

<sup>2</sup> Department of Geology, Shiraz Branch, Islamic Azad University, Shiraz, Iran, <https://orcid.org/0000-0002-2226-8433>, Email: dr.asadi.abdolmajid20@gmail.com

<sup>3</sup> Department of Geology, Shiraz Branch, Islamic Azad University, Shiraz, Iran.

<sup>4</sup> Department of Geology, Tehran North Branch, Islamic Azad University, Tehran, Iran.

Special resistivity methods are among the most widely used geophysical methods and one of the tools for identifying subsurface structures - more diverse than other geophysical methods. The variety of these methods has made it possible for them to be used in various studies, such as mining exploration, hydrogeology, geotechnics, ecology and engineering. In engineering studies, this method can be used to find subsurface cavities, faults, joints, sources of water and soil pollution, and the recognition of buried old buildings (Damavandi et al., 2022).

### **Literature Review**

In a geoelectrical method, the induced electric current is conducted into the ground by the electrodes and then the potential difference between different points is measured. Recording the potential differences between different locations leads to the identification of petrophysical properties and determining anisotropy in different directions. This method is the best ones in differentiating the underground layers; and regarding their special resistivity and thickness, being portable, easy to use, and cost effective, they are of the most powerful exploration methods (Ako & Olorunfemi, 1989). A geoelectrical operation is performed in two ways: vertical electric sounding and horizontal profiling (Kolagari, 2010). In geoelectrical

#### *Geographic location and access routes of the area under study*

The study area is located in Fars in north of west of Shiraz and north east of Sepidan, Beyza.

soundings, deep variations in special resistivity and layering are studied using arrays increasing the distance between electrodes or all of them symmetrically (Aghanabati, 2004). Special resistivity values are plotted considering distance and on algorithmic graphs (both logarithmic axes). Although some methods have been proposed for interpreting the slope of the layers, geoelectrical sounding works well only when the interfaces of the layers are horizontal (Milsom, 1989). In these methods, there are four types of conventional electrode arrays including simple, wenner, polar-polar, and Schlumberger (Yadav & Abolfazli, 1998). From among these four arrays, Schlumberger array is widely used in electrical explorations. For example, vertical sounding with Schlumberger array is the most common and most useful geophysical method in groundwater exploration studies (Ghalamkari et al., 2019). In this array, 4 electrodes (current and potential) are positioned along a straight line, so that the potential electrodes are interposed to each other between the current electrodes so that the centers of the current and potential electrodes overlap (Reynold, 1997). In this study, the geoelectrical method was used to identify the fault path and layer separation in specified locations and the effect of faults of the area on the layers using special electrical resistivity values in Schlumberger array.

### **Methodology**

Beyza region is a relatively large plain surrounded by the highlands from the north, south and west and is connected to Marvdasht Plain from east (Figure 1).

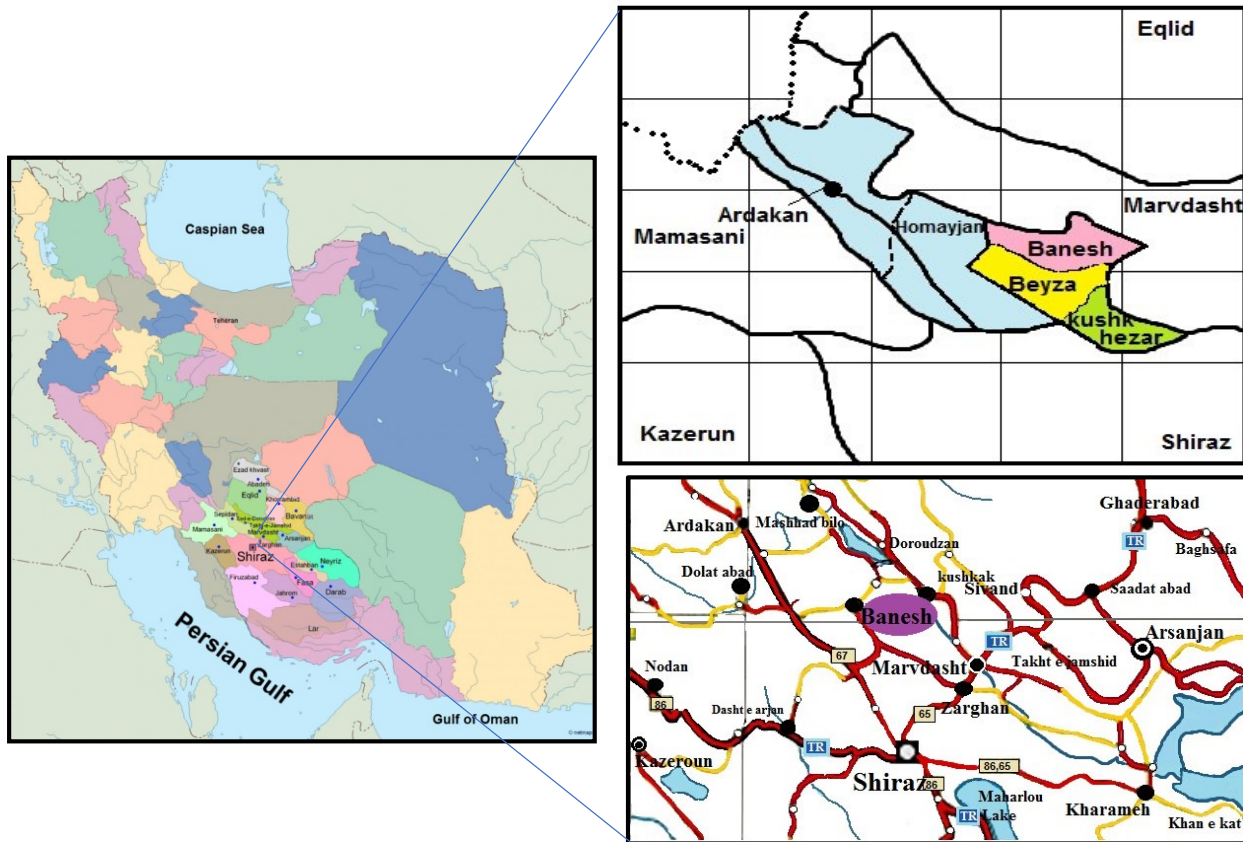


**Figure 1.** The Geographic location of Banesh and its access routes

## Results

### *Geology and tectonic of the area*

The study area is located in the Zagros active fold and thrust belt (FTB) tectonic unit according to Iran's tectonic division (Berberian, 1976). As the largest structural zone of Iran, the Zagros FTB has formed due to the collision of the Arabic plate and plateau of Iran in the late Tertiary (Stocklin, 1968). As mountain ranges with an approximate length of 1800 km and is located on the peaceful Arabian continental platform (Hessami, 2001). The arrays and movement of the Arabic plate in the south affect Iranian tectonic units and Eurasia in the north, creating various trends in different parts (Aghanabati, 2004). Convergence between continental plates often ends in the formation of FTBs. The upper sedimentary phanerozoic cover

of Zagros undergoes deformation during neogene collision orogeny. This deformation is manifested in the form of stretched and open folds and some thrusts. Earth shapes in the Zagros are essentially structural. Many of the folds in Zagros are asymmetric, so that their axial surfaces are towards the north and northeast (Berberian, 1995). The slope of the south and southwest ridges are more and in some cases close to the vertical, turned back or faulted (Berberian, 1994). The study area is in the faulted Zagros according to geologically divisions, and the formations of Sarvak, Gourpei, Fahlian, Gadvan, Darian and Kajdomi have outcrops in it as old as Cretaceous. Coupled with these formations, the present conglomerate and the recent quaternary alluvial and sediments cover a vast area. Due to the quaternary

sedimentary cover, the effects of fault, joint and fracture remain blind. This area is surrounded by Sangpahn Hignlands, Mount Ali Yaghi in the north, Mount Maal Amir in the northeast, Mount Sangpahn in the northwest and Mount Takht-e Sang-e-Olia in the south and south-east. The main faults and some anticlines are seen at these heights. The faults are on the border of the mountains with a dangling plain. Right-slip faults have caused some distortions along mountains and topographic landscapes. Quantitative geomorphic indexes show that the region can be divided into two different sections.

Although elevation in the northern part seems to be higher than the erosion rate, due to ultrahigh syncline in the southern half, the severity of the erosion is higher. Studies show that the study area in the Beyza Plain is the result of gravitational tectonic processes. In this area, a tensile phase has happened following Pasadenian orogeny phase with severe alluvium. Thus, quaternary sediments cover numerous folds in the plains with the thickness from 50 to 300 meters. Geophysical data and aeromagnetic maps are in line with this (Shahsavari, 2003) (Figure 2).

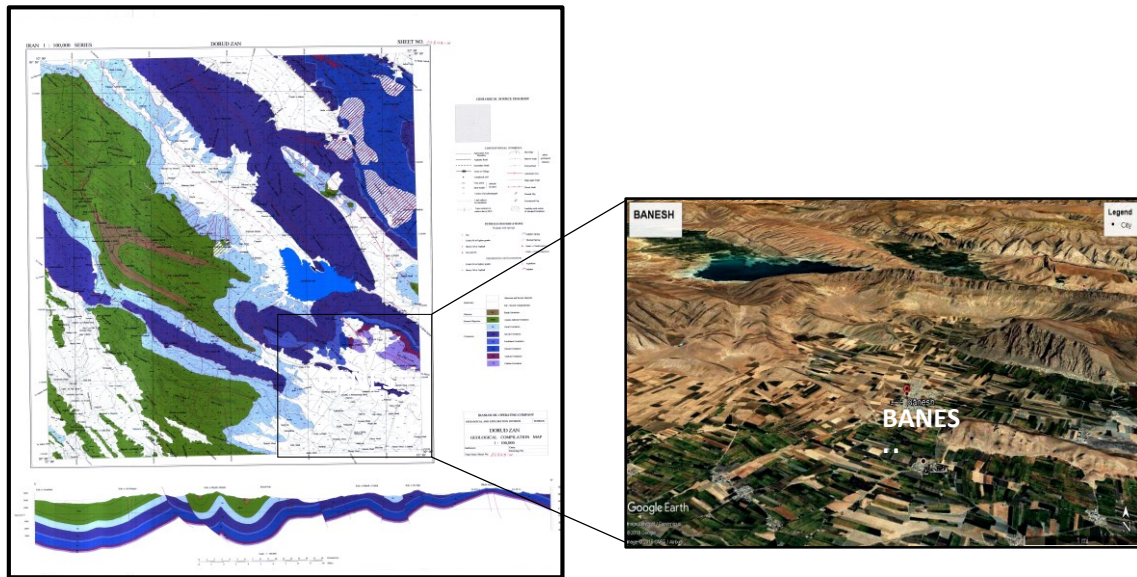


Figure 2. The location of Banesh study area on satellite imagery and geological map

## Discussion

In the first stage, any study records connected to the region and the subject matter, including books, papers, reports, and so on were collected and examined. Then, by studying geological and topographic maps, aerial imagery and satellite imagery, the geology and the tectonics of the study area were obtained. In the complementary stage, using a 30-meter digital elevation model, 1: 100,000 and 1: 25000 geological maps of

Beyza, and Global Mapper, ... we accurately identified the structures, fault and ground evidence construction of the region. In completing the above studies, common geophysical methods were used to confirm the evidence of tectonic and geological evidence of the presence of faults in the region – Schlumberger array was selected in this study. In doing so, field observations including measuring



and determining the position of the profile of the soundings in the designated sites (30 vertical soundings in the region) and reading the apparent resistivity of the geological layers (10 profiles based on the data collected) were done using geoelectrical device. Then, data were

analyzed and the results were interpreted (Figure 3). Finally, the blind faults were identified with the aggregation of rupture and joint studies, geophysical data, and geological and tectonic evidence. Several station and section profiles and pseudo-sections have been reviewed.

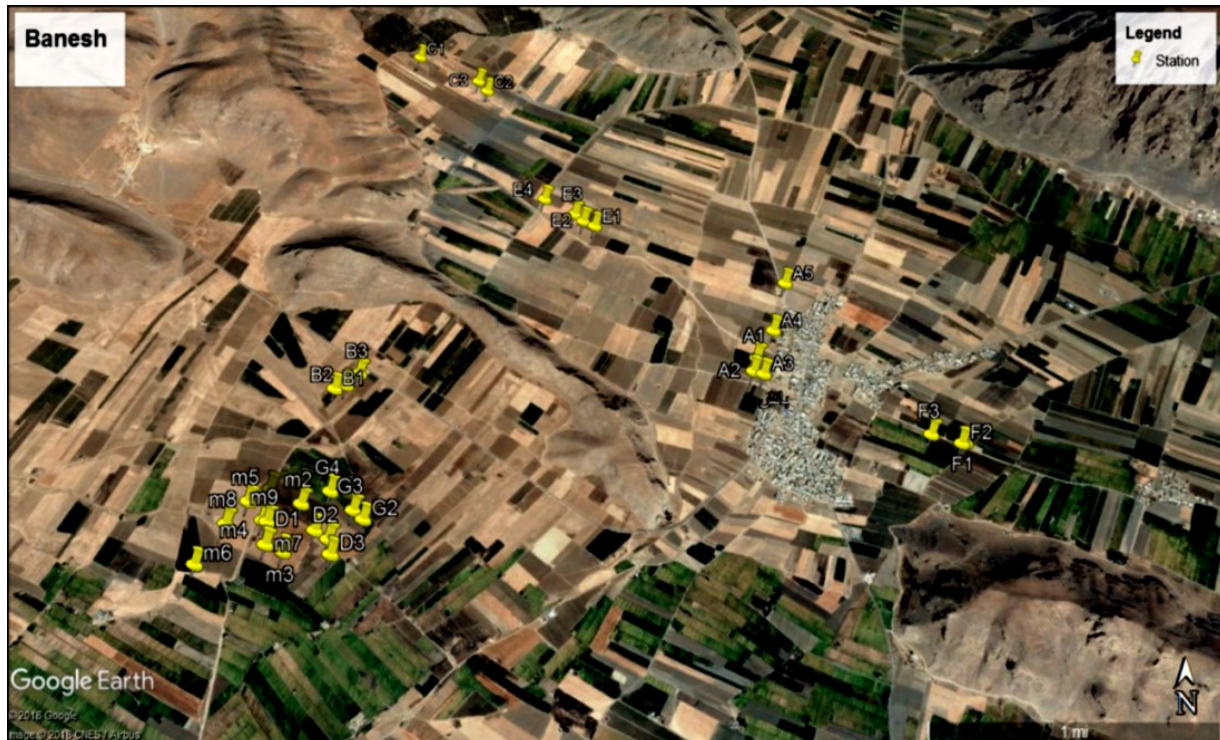


**Figure 3.** Sounding-stations location on satellite images (Google Earth)

### *Examining apparent resistivity graph*

Examining apparent resistivity graph of A5 and B2 stations shows that resistivity changes at these stations initially has decreasing then severely increasing trends and at Station E3, the overall resistivity trend is decreasing. Due to the crossing of the crushed zone from these stations in the deep sections, the presence of the crushed zone is seen in the graph. In addition, at Station B2, the penetration of moisture from the surface to the lower parts has caused drastic changes to resistivity, and at Station E3, the loss of resistivity in the deep parts was due to the

fracture of the stone floor and the transfer of moisture from the surface to the depth. Studying the apparent resistivity graph of Station C1 shows that the resistivity at the surface to the semi-deep part has had an increasing trend and then decreasing, and at Station G1 and M8 stations, resistivity increases gradually from surface to depth. The gradual increase resistivity from surface to depth at Station G1 indicates distancing from the crushed zone and the presence of a natural process of increasing resistivity from surface to depth, and at Station M8 in very deep parts, the sharp increase in

resistivity is due to changes in formations. The minimum number of layers at all stations is 3 layers and at Station M8 4 layers (Figure 4).

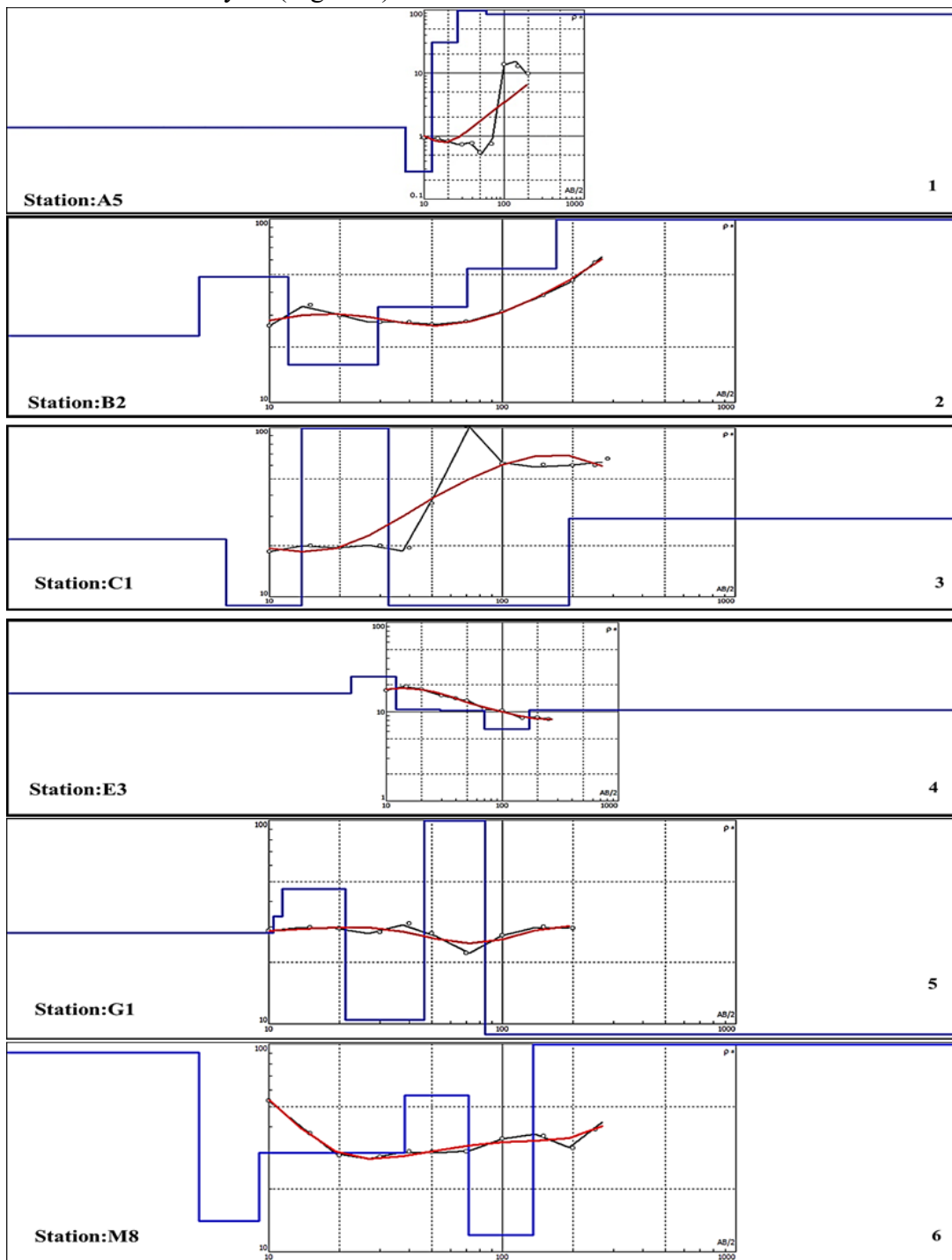


Figure 4. Sample apparent resistivity graphs from each profile

*Examining pseudo cross-section curves*

The geoelectrical pseudo cross-section curves show the distribution of the apparent electrical



resistivity at a deep cross-section along a profile. For the preparation of pseudo cross-sections, after flattening and before the interpretation of the field sounding curves, one should plot the apparent electrical resistivity values of sounding

of each profile against half the length of the current electrodes ( $AB/2$ ) (Asl et al., 2015). (Figure 5) shows the geoelectrical pseudo cross-sections of profile G as an example.

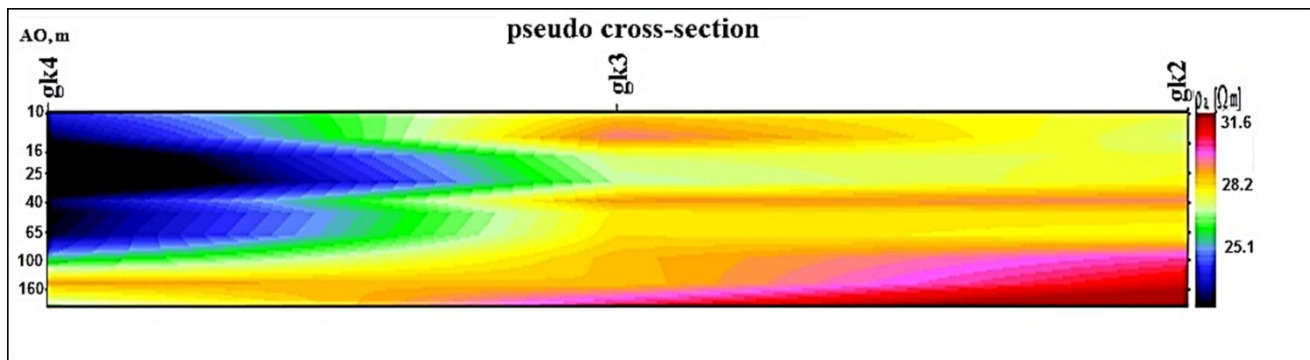


**Figure 5.** Geoelectrical pseudo cross-section of profile G

The study of pseudo cross-section and cross-sections of profile G shows that stations G2, G3 and G4 are limestone. The increase in resistivity, especially at stations GK2 and GK3, confirms the idea above, but this increase is extremely weak, especially at all three stations GK4, GK3 and GK2 and has occurred with slight slope increase. The reason for this is the crushed zone and fault from all three stations mentioned above. In other words, despite the existence of limestone rock from any of the 3 stations, the crushed zone has made it possible to easily penetrate the moisture in the deep parts and consequently reduce the severity of the increase in resistivity, especially in the actual sections. Thus, one can consider that the crushed fault zone passes through all three stations.

#### *Geoelectrical cross-sections*

After interpretation of the sounding graphs the catheter curves and determining the real depth separation and electrical resistivity of the sub-layers in each profile, one can plot the

geoelectrical cross-section of that profile. The geoelectrical cross-section is a vertical section of the sub-surface geoelectrical layers whose horizontal axis is the horizontal distances of the soundings relative to each other and the vertical axis is the depth of the layers. The layers are separated from each other according to the real special resistivity. (Figure 6) shows the geoelectrical cross-section of profile A resulting from the A5-A3-A2 sounding as an example. This cross-section shows that in all three stations, despite the presence of limestone, resistivity of the surface from the surface to the depth not only does not show a slight increase, but rather a slight decrease compared to the limestone rock. Thus, due to the passing of the crushed zone and the penetration of moisture into the deep parts of the rock, despite the presence of lime formation in deep sections, the decrease in especially indicates the passage of the crushed zone from all three stations. In other words, each of the three stations can be divided into a crushed zone and a fault that controls the groundwater.

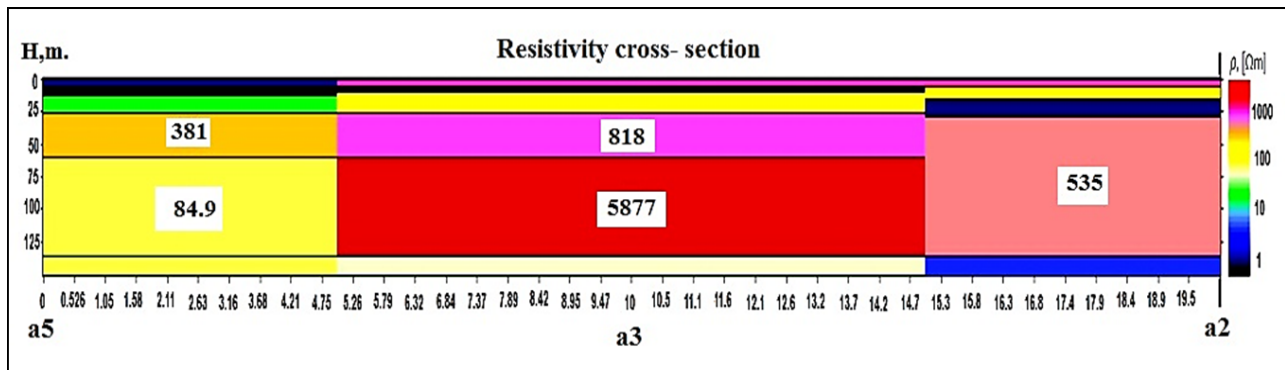


Figure 6. Geoelectrical cross-section of profile A

Studying pseudo cross-sectional and the cross-section of the profile stations of (Figure 7) shows that the limestone rock is well visible at all stations, but this floor rock in the A4 and F3 station has been severely crushed. Hence, unlike other stations, increasing resistivity in these two stations is less visible. In other words, due to the pass of the crushed zone from the stations, increase in resistivity occurs slowly. Additionally, at Station E3, due to the presence of sub-faults from this station, resistivity

changes show a decrease in the resistivity in the stone floor compared to other stations. In other words, despite the increase in resistivity at stations near, the crushed zone passing from Station E3 and the effect of this zone on the location of Station E2 have reduced the resistivity to the floor of Station E2 to some extent. Thus, the fault zone seems to have been cut diagonally along the pseudo cross-section and the above cross-section.

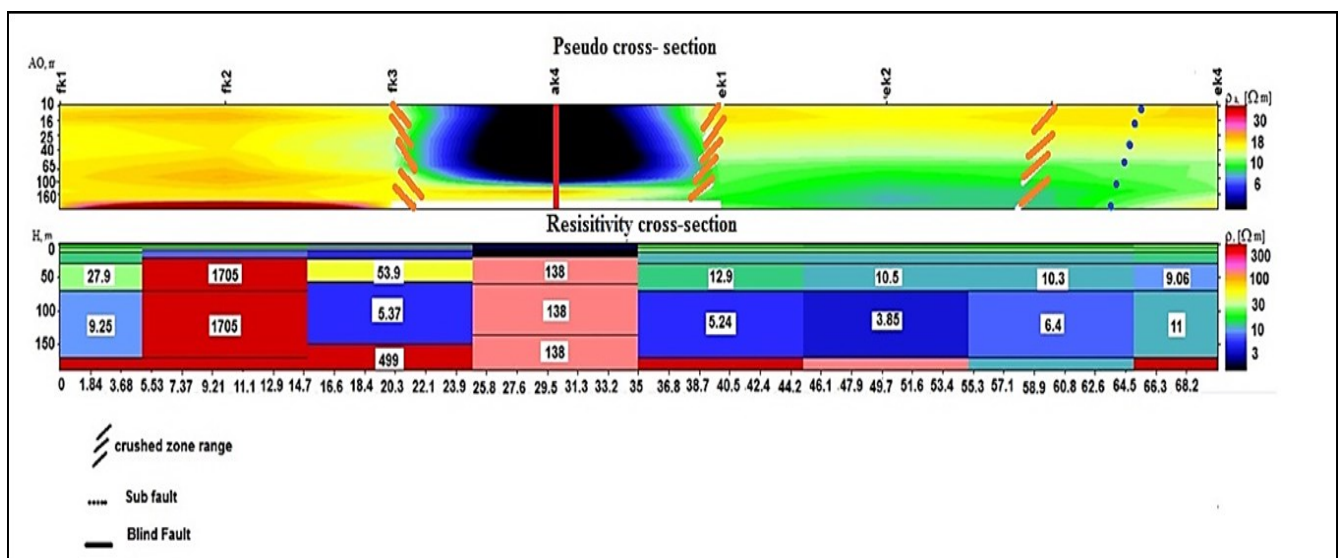


Figure 7. The cross-section and pseudo cross-section

(Figure 7), the cross-section and pseudo cross-section of the sample profile and the position of

the blind faults identified and the crushed areas on it at Station a4, the main fault, and the crushed



due to the covering of alluvial quaternary deposits, became possible by this method. The examinations show the floor limestone rock in all studied stations. In addition, studies well show that in stations where a fault zone has passed or the stations is near the crushed and faulted zones, the reduction in apparent resistivity is observed despite the floor limestone. Moreover, moisture penetration is easily made possible from the surface to the depth due to the crushed zone. For example, at G stations, where the pass of the fault and the crushed fault is accompanied by displacement, the effect of the crushed zone is such that has led to the penetration of moisture from the surface parts to the deep parts and decrease in the resistivity compared to the neighboring stations. Studies show the pass of fault zone from stations A1 to A5 is responsible for conducting groundwater in the area, and the pass of two thrust fault zones from the floor stone of stations B1 and B2 is easily seen. In addition, in stations E1 and E3, some diagonal sub-faults were seen.

### **Conflict of interest**

The authors declare that they have no conflict of interest.

### **References**

- Telford WM. & Geldart LP. & Sheriff RE. (1990). Applied Geophysics. 2nd Edition, Cambridge University Press, Cambridge. <https://doi.org/10.1017/CBO9781139167932>
- Azadi A. & Hessami K. & Javan-Doloei G. (2010). Integrated geophysical methods for determining geometry of the Kahrizak Fault, Tehran, Iran, Natural Hazards, 54(3): 813-825. <https://doi.org/10.1007/s11069-010-9506-9>
- Takahashi R. (2014). Geophysics for the Mineral Exploration Geoscientist Authors: by Michael Dentith and Stephen T. Mudge Publisher: Cambridge University Press Price. <https://doi.org/10.1111/rge.12057>
- Damavandi K. & Abedi M. & Norouzi GH. & Mojarab M. (2022). Geoelectrical characterization of a landslide surface for investigating hazard potency, a case study in the Tehran- North freeway, Iran. International Journal of Mining and Geo-Engineering, 56(4): 339-347. <https://doi.org/10.22059/ijmge.2022.340800.594958>
- Ako BD. & Olorunfemi MO. (1989). Geoelectric survey for groundwater in the Newer Basalts of Vom, Plateau State. Journal of Mining and Geology, 25(1): 247-250.

### **Additional Information and Declarations Funding**

*There is no funding.*

### **Grant Disclosures**

There was no grant funder for this study.

### **Competing Interests**

The author declares there is no competing interests, regarding the publication of this manuscript

### **Author Contributions**

Raheleh Farhang and Abdolmajid Asadi developed the study concept and design. Kouros Yazdjerdi acquired the data. Mohsen Pourkermani and Raheleh Farhang analyzed and interpreted the data, and wrote the first draft of the manuscript. All authors contributed to the intellectual content, manuscript editing and read and approved the final manuscript.

### **Ethics Statement**

Shiraz Branch, Islamic Azad University, Shiraz, Iran



- Kolagari AA. (2010). Principles of Geophysical Exploration. Publisher Tabriz University.
- Aghanabati A. (2004). Geology of Iran. Publisher Geological Survey of Iran.
- Milsom J. (1989). Field Geophysics. Geological Society of London Handbook Series.  
<https://www.abebooks.com/9780335152070/Field-geophysics-Geological-Society-London-0335152074/plp>
- Yadav GS. & Abolfazli H. (1998). Geoelectrical soundings and their relationship to hydraulic parameters in semiarid regions of Jalore, northwestern India. Journal of Applied Geophysics, 39(1): 35-51. [https://doi.org/10.1016/S0926-9851\(98\)00003-2](https://doi.org/10.1016/S0926-9851(98)00003-2)
- Ghalamkari S. & Asadi A. & Pourkermani M. & Mazdarani A. (2019). Pourkermani M. Geoelectric assessment of groundwater aquifers at RONIZ area, Southeastern SHIRAZ, IRAN. Geomech. Geophys. Geo-energ. Geo-resour, 5(1): 425-436. <https://doi.org/10.1007/s40948-019-00121-4>
- Reynolds JM. (1997). An Introduction to Applied and Environmental Geophysics Publisher Wiley; 2nd edition. <https://www.amazon.com/Introduction-Applied-Environmental-Geophysics/dp/0471485365>
- Berberian M. (1976). Contribution to the Seismotectonics of Iran (Part II), G. S. I., Rep.
- Stocklin J. (1968). Structural History and Tectonic of Iran: A Review. American Association of Petroleum Geologists Bulletin, USA, 52(1): 1229-1258. <https://doi.org/10.1306/5D25C4A5-16C1-11D7-8645000102C1865D>
- Hessami K. (2001). The Significance of Strike-Slip Faulting in the Basement of the Zagros Sold and Thrust Belt. Journal of Petroleum Geology, 24(1): 5-28. <https://doi.org/10.1111/j.1747-5457.2001.tb00659.x>
- Berberian M. (1995). Master Blind Thrust Faults Hidden under the Zagros Folds: Active Basement Tectonics and Surface Morphotectonics. Tectonophysics Journal, 241(1): 193-224. <https://scirp.org/reference/referencespapers.aspx?referenceid=1859078>
- Berberian M. (1994). Natural Hazards and the First Earthquake Catalogue of Iran. Vol. 1: Historical Hazards in Iran Prior to 1900. A UNESCO/IIIES Publication during UN/IDNDR: International Institute of Earthquake Engineering and Seismology, Tehran, Iran. [https://www.scirp.org/\(S\(i43dyn45teexjx455qlt3d2q\)\)/reference/ReferencesPapers.aspx?ReferenceID=1769050](https://www.scirp.org/(S(i43dyn45teexjx455qlt3d2q))/reference/ReferencesPapers.aspx?ReferenceID=1769050)
- Shahsavari A. (2003). Morphotectonic Analysis of Beyza Plain, MA Thesis. Shiraz University.
- Asl MM. & Pour HJ. & Mehramuz M. (2015), Detection of faults position and possible crushed zones by using electrical resistivity and microgravity methods: Application to the Lar Dam area, Iran. Arab J Geosci, 8(1): 1497-1512. <https://doi.org/10.1007/s12517-013-1214-9>
- Shaw JH. & Shearer PM. (1999). An Elusive Blind-Thrust Fault Beneath Metropolitan Los Angeles. Science, 283(5407): 1516-1518. <https://doi.org/10.1126/science.283.5407.1516>